Applied Mathematics Letters 157 (2024) 109170

Contents lists available at ScienceDirect

Applied Mathematics Letters

journal homepage: www.elsevier.com/locate/aml

Regular article

Noisy tensor recovery via nonconvex optimization with theoretical recoverability

Meng Ding [a], Jinghua Yang [b,*], Jin-Jin Mei [c]

[a] School of Mathematics, Southwest Jiaotong University, China
[b] School of Information Science and Technology, Southwest Jiaotong University, China
[c] School of Mathematics and Statistics, Fuyang Normal University, China

ARTICLE INFO

Keywords:
Noisy tensor recovery
Sparsity
ℓ_1 regularization
Theoretical recoverability

ABSTRACT

Noisy tensor recovery aims to estimate underlying low-rank tensors from the noisy observations. Besides the sparse noise, tensor data can also be corrupted by the small dense noise. Existing methods typically use the Frobenius norm to handle the small dense noise. In this work, we build a new nonconvex model to decompose the low-rank and sparse components. To be specific, we employ the ℓ_1 norm to handle the small dense noise term, the ℓ_0 'norm' to enforce the sparse outliers, and the tensor nuclear norm to model the underlying low-rank tensor. We develop an effective alternating minimization-based algorithm. Under certain conditions, we prove that the proposed method has a high probability of exactly recovering low-rank and sparse tensors. Numerical experiments showcase the advantage of our method.

1. Introduction

Due to environmental factors or transmission equipment interference, the collected data is often contaminated by noise. Robust principal component analysis (RPCA) is one of the most critical and fundamental approaches in data recovery [1–3]. Given the noisy data $\boldsymbol{X} \in \mathbb{R}^{n_1 \times n_2}$, RPCA aims to estimate a low-rank matrix $\boldsymbol{L}_0$ that captures the underlying structure of $\boldsymbol{X}$ and a sparse matrix $\boldsymbol{E}_0$ that represents the sparse noise. Mathematically, RPCA [1] is formulated as

$$\min_{\boldsymbol{L},\boldsymbol{E}} \ \|\boldsymbol{L}\|_* + \lambda\|\boldsymbol{E}\|_1, \quad \text{s.t. } \boldsymbol{X} = \boldsymbol{L} + \boldsymbol{E}. \tag{1}$$

Here $\|\boldsymbol{L}\|_*$ and $\|\boldsymbol{E}\|_1$ respectively represent the nuclear norm and the ℓ_1 norm. Under suitable assumptions [1], one can exactly recover $\boldsymbol{L}_0$ and $\boldsymbol{E}_0$ with a high probability by (1). In addition to the sparse corruption, $\boldsymbol{X}$ may also be damaged by the small dense noise $\boldsymbol{N}$, resulting in $\boldsymbol{X} = \boldsymbol{L}_0 + \boldsymbol{E}_0 + \boldsymbol{N}$. A number of works have been proposed to handle the dense noise; see references therein [4–8].

The aforementioned methods are primarily designed for matrix data and achieve the promising performance. Nevertheless, in real applications, many data are multi-dimensional arrays or tensors [9–13]. For example, multi-spectral images can be formed as 3D tensors with one spectral and two spatial dimensions; color videos, known as 4D tensors, have one color channel, two spatial and one time dimensions. Applying matrix-based methods to handle the multi-dimensional data, one should flatten tensor data into a matrix, resulting in destroying the multi-dimensional structure of tensor data and then limiting recovery performance. Therefore, one natural and effective strategy is to directly handle the multi-dimensional data to keep the intrinsic structure.

Given a corrupted 3D tensor $\mathcal{X} = \mathcal{L}_0 + \mathcal{E}_0 \in \mathbb{R}^{n_1 \times n_2 \times n_3}$, robust tensor recovery aims to identify the underlying data $\mathcal{L}_0$ and the sparse noise $\mathcal{E}_0$. The tensor data in practice, e.g., multi-spectral images and videos, are generally low-rank due to the intrinsic

* Corresponding author.
E-mail addresses: dingmeng56@swjtu.edu.cn (M. Ding), yangjinghua110@126.com (J. Yang), meijinjin666@126.com (J.-J. Mei).

https://doi.org/10.1016/j.aml.2024.109170
Received 17 April 2024; Received in revised form 24 May 2024; Accepted 24 May 2024
Available online 4 June 2024

correlations and redundancy. Many tensor decompositions and the corresponding ranks are utilized to explore the global low-rank prior, such as the most representative CANDECOMP/PARAFAC [14] and Tucker decomposition [15]. The work in [16] recovered the underlying low-rank tensor $\mathcal{L}_0$ by minimizing Tucker rank [17]. Similar to the matrix data, besides the outliers, there is also the small dense tensor noise $\mathcal{N}$. To proceed, the work in [18] studied the noisy Tucker tensor decomposition as follows:

$$\min_{\mathcal{L},\mathcal{E}} \ \frac{1}{2}\|\mathcal{X}-\mathcal{L}-\mathcal{E}\|_F^2+\mu\|\mathcal{L}\|_{\text{SNN}}+\lambda\|\mathcal{E}\|_1, \tag{2}$$

where $\|\mathcal{L}\|_{\text{SNN}}$ denotes the sum of nuclear norm (SNN) [19] (the convex envelope of Tucker rank), i.e., $\|\mathcal{L}\|_{\text{SNN}}=\sum_{i=1}^{3}\|\boldsymbol{L}_{[i]}\|_*$, where $\boldsymbol{L}_{[i]}$ represents the unfolding matrix [17] of tensor $\mathcal{L}$ along the ith mode, and $\|\boldsymbol{L}\|_*$ denotes the matrix nuclear norm. Recently, the tensor singular value decomposition (TSVD) is proposed [20], and the corresponding tensor tubal rank [9,20] has achieved promising performance [9,21,22]. The work in [9] studied its convex surrogate, tensor nuclear norm (TNN), and proposed tensor RPCA (TRPCA) as

$$\min_{\mathcal{L},\mathcal{E}} \ \|\mathcal{L}\|_*+\lambda\|\mathcal{E}\|_1, \text{s.t. } \mathcal{X}=\mathcal{L}+\mathcal{E}, \tag{3}$$

where $\|\mathcal{L}\|_*$ represents the TNN (see Definition 3). Under certain conditions [9], one can exactly recover the ground-truth by solving (3). To handle the small dense noise, the work in [23] proposed the following TNN-based model

$$\min_{\mathcal{L},\mathcal{E}} \ \frac{1}{2}\|\mathcal{X}-\mathcal{L}-\mathcal{E}\|_F^2+\mu\|\mathcal{L}\|_*+\lambda\|\mathcal{E}\|_1. \tag{4}$$

In the fidelity items of (2) and (4), the authors used the Frobenius norm to model the small dense noise, which is reasonable. However, it may not identify all sparse outliers when updating the sparse tensor, leading to the performance degradation.

In this work, we develop a new nonconvex model for estimating the underlying low-rank tensor and the sparse outliers from the noisy observation. Specifically, we directly utilize the ℓ_0 'norm' to model the sparsity of outliers. More importantly, we employ the ℓ_1 norm rather than the Frobenius norm for the additive dense noise to help handle the unidentified outliers. For the nonconvex model, we propose an alternating minimization optimization algorithm. Under certain conditions, we provide the exact recovery for the sparse tensor and low-rank tensor. Experiments demonstrate the outstanding recovery performance of our method over classical baselines.

2. Notations and preliminaries

We briefly present the related notations (shown in Table 1) and preliminaries.

Definition 1 (*T-product [24]*)**.** Given two $n_1\times n_2\times n_3$ and $n_2\times n_4\times n_3$ tensors $\mathcal{A}$ and $\mathcal{B}$, the t-product $\mathcal{A}*\mathcal{B}$ yields a tensor $\mathcal{C}\in\mathbb{R}^{n_1\times n_4\times n_3}$, whose (i,m)th tube is computed by $\mathcal{C}(i,m,:)=\sum_{j=1}^{n_2}\mathcal{A}(i,j,:)\star\mathcal{B}(j,m,:)$, where $\star$ is the circular convolution of two vectors.

Definition 2 (*TSVD and Tensor Tubal Rank [20]*)**.** Assuming a tensor $\mathcal{X}$ of size $n_1\times n_2\times n_3$, its TSVD is

$$\mathcal{X}=\mathcal{U}*\mathcal{S}*\mathcal{V}^H,$$

where $\mathcal{S}$ is a $n_1\times n_2\times n_3$ f-diagonal tensor, and two tensors $\mathcal{U}$ ($n_1\times n_1\times n_3$) and $\mathcal{V}$ ($n_2\times n_2\times n_3$) are orthogonal. Then the tensor tubal rank is $\text{rank}_t(\mathcal{X})=\#\{i:\mathcal{S}(i,i,:)\neq 0\}$. The rank-$r$ skinny TSVD of $\mathcal{X}$ is $\mathcal{X}=\mathcal{U}_r*\mathcal{S}_r*\mathcal{V}_r^H$, where $\mathcal{U}_r=\mathcal{U}(:,1:r,:)$, $\mathcal{S}_r=\mathcal{S}(1:r,1:r,:)$, and $\mathcal{V}_r=\mathcal{V}(:,1:r,:)$.

The definitions of *conjugate transpose*, *f-diagonal tensor*, and *orthogonal tensor* are listed in the supplement materials due to the page limitation.

Definition 3 (*TNN [9]*)**.** Assume $\mathcal{X}\in\mathbb{R}^{n_1\times n_2\times n_3}$ can be decomposed as $\mathcal{X}=\mathcal{U}*\mathcal{S}*\mathcal{V}^H$, its TNN is defined as $\|\mathcal{X}\|_*=\sum_{i=1}^{\text{rank}_t(\mathcal{X})}\mathcal{S}(i,i,1)$.

3. Sparse TRPCA

3.1. Proposed model and algorithm

We study the following nonconvex minimization problem:

$$\min_{\mathcal{L},\mathcal{E}} \ \lambda\|\mathcal{X}-\mathcal{L}-\mathcal{E}\|_1+\|\mathcal{L}\|_*+\theta\|\mathcal{E}\|_0. \tag{5}$$

Compared with (4), we directly utilize the ℓ_0 'norm' to enforce the sparse $\mathcal{E}_0$. Another main difference is that we substitute the Frobenius norm with ℓ_1 norm to handle the small dense noise. But this substitute not only helps to identify outliers and improve the recovery performance, but also admits the theoretical guarantee, which will be discussed later. We adopt the alternating minimization method to alternately update the variables in (5), which is referred as Sparse TRPCA (STRPCA).

Update $\mathcal{L}^{(t+1)}$: Fixed $\mathcal{E}^{(t)}$, we minimize the following problem

$$\mathcal{L}^{(t+1)}=\underset{\mathcal{L}}{\text{argmin}} \ \|\mathcal{L}\|_*+\lambda\|\mathcal{X}-\mathcal{L}-\mathcal{E}^{(t)}\|_1. \tag{6}$$

Update $\mathcal{E}^{(t+1)}$: Fixed $\mathcal{L}^{(t+1)}$, we minimize the following problem

$$\mathcal{E}^{(t+1)} = \underset{\mathcal{E}}{\operatorname{argmin}}\ \theta\|\mathcal{E}\|_0 + \lambda\|\mathcal{X} - \mathcal{L}^{(t+1)} - \mathcal{E}\|_1. \tag{7}$$

Note that for the first term in (5), using Frobenius norm may be more suitable than ℓ_1 norm, especially when the observed $\mathcal{X}$ is damaged by Gaussian noise. However, one should point out that in the step of updating $\mathcal{L}$ (6) of each iteration, we want to remove sparse outliers, while it cannot be expected that all outliers are totally detected in the previous loop. It is highly probable that some outliers still remain. Therefore, it is advisable to use the ℓ_1 norm instead of the Frobenius norm.

In the first iteration, we have no information about the sparse outlier, so we simply set $\mathcal{E}^{(0)} = 0$. Therefore, updating $\mathcal{L}$ at first iteration turns to solve

$$\min_{\mathcal{L}}\ \|\mathcal{L}\|_* + \lambda\|\mathcal{X} - \mathcal{L}\|_1. \tag{8}$$

One can easily get that (8) is actually TRPCA in (3). Next, we give the detailed solver for each subproblem. In updating $\mathcal{L}$, the convex problem can be regarded as TRPCA with $\mathcal{X} - \mathcal{E}^{(t)}$. The augmented Lagrange multiplier approach [25] is employed to handle the $\mathcal{L}$-subproblem. In updating $\mathcal{E}$, we can directly obtain its closed-form solution according to [7]:

$$[\mathcal{E}^{(t+1)}]_{ijk} = \begin{cases} 0, & |[\mathcal{X} - \mathcal{L}^{(t+1)}]_{ijk}| \le \theta/\lambda, \\ [\mathcal{X} - \mathcal{L}^{(t+1)}]_{ijk}, & \text{otherwise.} \end{cases} \tag{9}$$

From (9), the entry $[\mathcal{X} - \mathcal{L}^{(t+1)}]_{ijk}$ will be identified as a sparse outlier if its absolute value exceeds the threshold θ/λ. We summarize the proposed method in Algorithm 1, which is shown in Appendix B of the supplemental materials. In future, we will analyze the convergence of our algorithm.

Complexity. The main computational cost of STRPCA is to update $\mathcal{L}$. Without loss of generality, assume $n_1 \ge n_2$. Computing $\mathcal{L}$ costs $\mathcal{O}(mn_3(n_1n_2^2 + n_1n_2\log n_3))$ [9], where m is the number of inner iterations of $\mathcal{L}$-subproblem. Practically, when updating $\mathcal{L}$ of the $(t+1)$th iteration, we utilize the previous $\mathcal{L}^{(t)}$ as the initialization, which can decrease the complexity cost of our method.

3.2. Theoretical recoverability

Here, we establish the theoretical recoverability of STRPCA when the observed tensor is not damaged by the dense noise. Let $\mathring{\mathfrak{e}}_i$ of size $n_1 \times 1 \times n_3$ represents the tensor column basis, whose $(i,1,1)$th entry is set to 1 and remaining entries are set to 0. Suppose that the rank-r skinny TSVD of $\mathcal{L}_0$ is $\mathcal{U}_r * \mathcal{S}_r * \mathcal{V}_r^{\mathrm{T}}$, then $\mathcal{L}_0$ satisfies the *tensor incoherence conditions* [9] with parameter μ_0 if

$$\max_{i=1,\dots,n_1} \|\mathcal{U}_r^H * \mathring{\mathfrak{e}}_i\|_F \le \sqrt{\frac{\mu_0 r}{n_1 n_3}},\quad \max_{j=1,\dots,n_2} \|\mathcal{V}_r^H * \mathring{\mathfrak{e}}_j\|_F \le \sqrt{\frac{\mu_0 r}{n_2 n_3}},\ \text{and}\ \|\mathcal{U}_r * \mathcal{V}_r^H\|_\infty \le \sqrt{\frac{\mu_0 r}{n_1 n_2 n_3^2}}. \tag{10}$$

Next, we establish the exact recovery property of STRPCA, which is proved in Appendix C of the supplemental materials.

Theorem 1. *Assume that $\mathcal{L}_0 \in \mathbb{R}^{n_1\times n_2\times n_3}$ satisfies the conditions (10). Assume that the support set Ω of $\mathcal{E}_0$ is uniformly distributed among all sets with a cardinality of m, and fixing any $\mathcal{M} \in \mathbb{R}^{n_1\times n_2\times n_3}$ of signs, $sgn([\mathcal{E}_0]_{ijk}) = [\mathcal{M}]_{ijk}$, $(i,j,k) \in \Omega$. Without loss of generality, assume $n_1 \ge n_2$. If there exist two constants $\rho_r, \rho_s > 0$, rank$(\mathcal{L}_0) \le \frac{\rho_r n_2 n_3}{\mu_0(\log(n_1 n_3))^2}$ and $m \le \rho_s n_1 n_2 n_3$, then STRPCA with $\lambda = \frac{1}{\sqrt{n_1 n_3}}$ and $0 < \theta < \frac{1}{\sqrt{n_1 n_3}} \min\{|[\mathcal{E}_0]_{ijk}| \ne 0\}$ exactly recovers $(\mathcal{L}_0, \mathcal{E}_0)$ in two iterations with a probability at least $1 - c_1(n_1 n_3)^{-c_2}$ with $c_1, c_2 > 0$.*

Remark. We should point that the exact recovery property analysis of our STRPCA is inspired by the results in [9]. Nonetheless, the optimization model of [9] is convex with one parameter, while the proposed model is nonconvex with two parameters. By the well-designed alternating optimization algorithm and the parameters settings, we prove that the proposed nonconvex optimization method can still exactly recover the low-rank and sparse components.

4. Simulations

In this section, we present numerical experiments using multi-spectral images (MSI)[1] and videos[2] to verify the advantage of our STRPCA. The baselines include Robust Tensor Decomposition via SNN (RTD-SNN) [18], TRPCA [9], Robust Tensor Decomposition via TNN (RTD-TNN) [23]. To better show the advantage of using ℓ_1 norm rather than Frobenius norm, we also compare with the method by using the ℓ_0 'norm' to replace ℓ_1 norm in (4), termed as RTD-TNNℓ_0.

Parameter Settings. The proposed STRPCA involves two parameters λ and θ. Empirically, we select the value of λ from a set $\{a/\sqrt{\max(n_1,n_2)n_3}\}$ where $a = [0.6 : 0.2 : 2]$ and the value of θ from $\{0.05, 0.1, 0.2, 0.3\}$. For baselines, we carefully tune the corresponding parameters following the baselines' suggestions to achieve the best results within the context of the experimental settings of this work. The detailed parameters settings of baselines are shown in Appendix D of the supplemental materials. All numerical results are averaged from 10 random trials.

MSI Recovery. The testing multi-spectral images include *Toy*, *Flowers*, and *Feathers* of size $256 \times 256 \times 31$. We randomly add the sparse noise with noise ratio (NR) = 0.3 and the white Gaussian noise with zero mean and variance 0.05. To measure the quality of recovery, we use two metrics, including the structural similarity (SSIM) [26] and the peak signal-to-noise ratio (PSNR).

Table 1
Notations.

Symbol	Explanation	Symbol	Explanation
x, $\boldsymbol{x}$	Scalar, vector	$\|\mathcal{X}\|_F$	Frobenius norm $\|\mathcal{X}\|_F = \sqrt{\sum_{i,j,k}[\mathcal{X}]_{ijk}^2}$
$\boldsymbol{X}$, $\mathcal{X}$	Matrix, tensor	$\|\mathcal{X}\|_0$	ℓ_0 'norm' $\|\mathcal{X}\|_0 = \#\{(i,j,k) : [\mathcal{X}]_{ijk} \neq 0\}$
$[\mathcal{X}]_{ijk}$	(i,j,k)th entry of $\mathcal{X} \in \mathbb{R}^{n_1 \times n_2 \times n_3}$	$\mathcal{X}^H$	Conjugate transpose $(n_2 \times n_1 \times n_3)$ of $\mathcal{X}$
$\|\mathcal{X}\|_1$	ℓ_1 norm $\|\mathcal{X}\|_1 = \sum_{i,j,k} \|[\mathcal{X}]_{ijk}\|$	sgn$(\cdot)$	Signum function

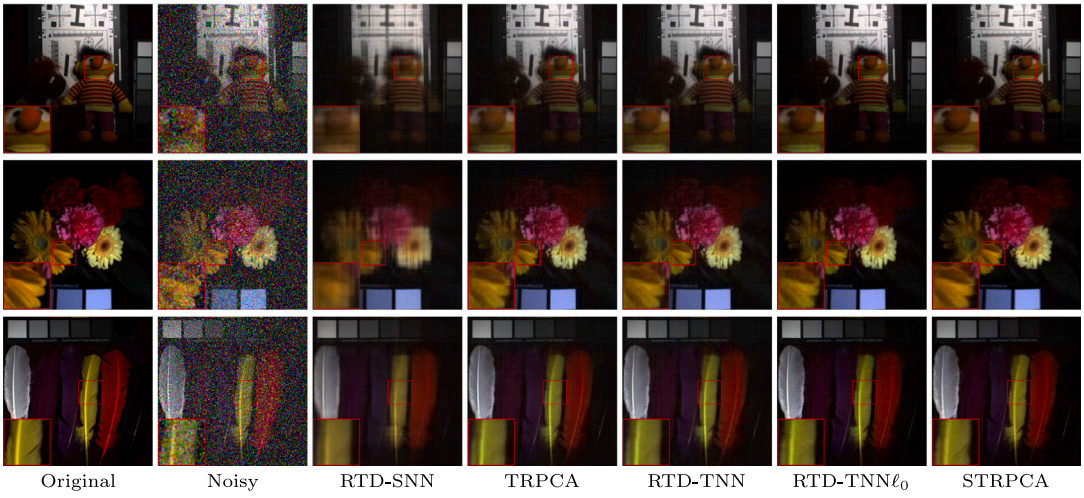

Fig. 1. Denoising results (R-G-B: 30-20-10 bands) on MSIs (from top to bottom: *Toy*, *Flowers*, and *Feathers*).

Table 2
Recovery performance (PSNR, SSIM) on three MSIs under NR=0.3.

MSIs	Metrics	Noisy	RTD-SNN	TRPCA	RTD-TNN	RTD-TNNℓ_0	STRPCA
Toy	PSNR	10.94	24.56	28.25	28.41	30.21	**31.72**
	SSIM	0.0892	0.6306	0.7016	0.6831	0.7725	**0.8762**
Flowers	PSNR	10.80	24.51	27.49	27.57	29.03	**30.40**
	SSIM	0.0598	0.5382	0.5561	0.5902	0.7056	**0.8101**
Feathers	PSNR	11.06	24.05	27.50	27.62	29.20	**29.59**
	SSIM	0.0719	0.6487	0.7145	0.7119	0.7427	**0.8529**

Fig. 1 presents the images estimated by all methods. One can see that all methods can reduce the noise, outputting less noise images compared to the observed ones. Nevertheless, one can see that RTD-SNN oversmooths the edges of recovered images. TRPCA and RTD-TNN lose the structures of images. The method RTD-TNNℓ_0 works well. In comparison, the proposed STRPCA performs better in preserving the sharp edges and smoothness of the recovered images. Note that the only difference between RTD-TNNℓ_0 and the proposed STRPCA is that replacing Frobenius norm, we employ the ℓ_1 norm on the small dense noise term. The denoising images demonstrate that this replacement can effectively reduce the noise and improve the recovered performance. The values of PSNR and SSIM listed in Table 2 also show that STRPCA performs better than baselines.

Video Background Modeling. We test STRPCA to separate the foreground and background from the videos. Due to the high correlation, the background of all frames generally admits the low-rank prior. The foreground contains a small amount of moving objects and thus admits the sparse prior. We choose two videos, including *Hall* of size 240 × 352 (spatial) × 80 (frame) and *Highway* of size 240 × 320 (spatial) × 100 (frame). Fig. 2 shows the visual effects of the foreground and background.

One can see that for *Hall*, there exist some ghosting of the person (at the left of the frame) in the backgrounds recovered by the baselines. The proposed STRPCA performs well in modeling the background. For *Highway*, all methods can effectively separate the background and foreground from the frame. However, our STRPCA can keep the details of background, better than baselines.

[1] https://www.cs.columbia.edu/CAVE/databases/multispectral/
[2] https://sbmi2015.na.icar.cnr.it/SBIdataset.html

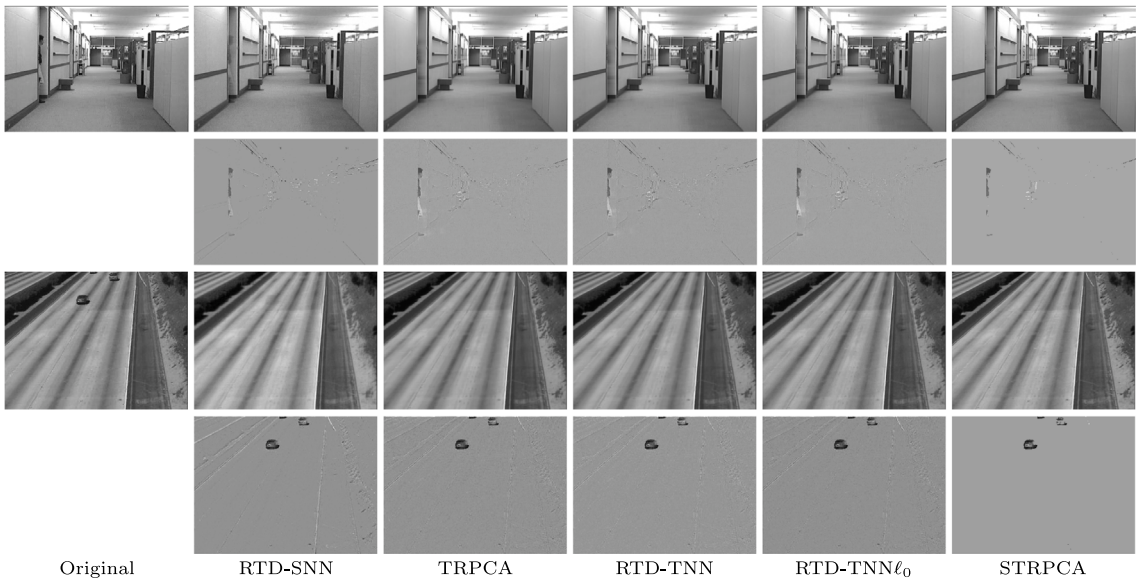

Fig. 2. The visual effects of the foreground and background of videos. First and second rows: the background and foreground of *Hall*; Third and fourth rows: the background and foreground of *Highway*.

5. Conclusions

We propose a new nonconvex optimization model for decomposing the low-rank tensor and sparse tensor from the observation that is also corrupted by the small dense noise. Different from the existing tensor-based methods, we impose ℓ_1 norm on the additive dense noise term. Under certain conditions, we establish the theoretical exact recovery guarantee. The promising performance of the proposed method is shown by the experiments on multi-spectral image recovery and video background modeling. One can use the nonconvex low-rank surrogate for further performance improvement and study the theoretical guarantee, which will be considered in our ongoing work.

Acknowledgments

The work was supported in part by NSFC, China (12201522 and 11901101), Natural Science Foundation of Sichuan Province, China (2024NSFSC1389 and 2024NSFSC1467), Natural Science Foundation of Anhui Province, China (1908085QA08), Fundamental Research Funds for the Central Universities, China (2682023CX069 and 2682024CX017), Natural Science Research Projects of Anhui Province (KJ2020A0535), and Young Talents Projects of Fuyang Normal University (rcxm202103).

Appendix A. Supplementary data

Supplementary material related to this article can be found online at https://doi.org/10.1016/j.aml.2024.109170.

References

[1] E.J. Candès, X. Li, Y. Ma, J. Wright, Robust principal component analysis? J. ACM 58 (3) (2011) 1–37.
[2] V. Chandrasekaran, S. Sanghavi, P.A. Parrilo, A.S. Willsky, Rank-sparsity incoherence for matrix decomposition, SIAM J. Optim. 21 (2) (2011) 572–596.
[3] Y. Peng, A. Ganesh, J. Wright, W. Xu, Y. Ma, RASL: Robust alignment by sparse and low-rank decomposition for linearly correlated images, IEEE Trans. Pattern Anal. Mach. Intell. 34 (11) (2012) 2233–2246.
[4] T. Zhou, D. Tao, GoDec: Randomized low-rank & sparse matrix decomposition in noisy case, in: Proc. ICML, 2011, pp. 33–40.
[5] Z. Zhou, X. Li, J. Wright, E. Candes, Y. Ma, Stable principal component pursuit, in: Proc. ISIT, 2010, pp. 1518–1522.
[6] D. Hsu, S.M. Kakade, T. Zhang, Robust matrix decomposition with sparse corruptions, IEEE Trans. Inform. Theory 57 (11) (2011) 7221–7234.
[7] J. Liu, P.C. Cosman, B.D. Rao, Robust linear regression via ℓ_0 regularization, IEEE Trans. Signal Process. 66 (3) (2018) 698–713.
[8] J. Liu, B.D. Rao, Robust PCA via ℓ_0-ℓ_1 regularization, IEEE Trans. Signal Process. 67 (2) (2019) 535–549.
[9] C. Lu, J. Feng, Y. Chen, W. Liu, Z. Lin, S. Yan, Tensor robust principal component analysis with a new tensor nuclear norm, IEEE Trans. Pattern Anal. Mach. Intell. 42 (4) (2020) 925–938.
[10] J. Liu, P. Musialski, P. Wonka, J. Ye, Tensor completion for estimating missing values in visual data, IEEE Trans. Pattern Anal. Mach. Intell. 35 (1) (2013) 208–220.
[11] Z. Qin, Z. Ming, L. Zhang, Singular value decomposition of third order quaternion tensors, Appl. Math. Lett. 123 (2022) 107597.
[12] M. Ding, X. Fu, T.-Z. Huang, J. Wang, X.-L. Zhao, Hyperspectral super-resolution via interpretable block-term tensor modeling, IEEE J. Sel. Top. Signal Process. 15 (3) (2021) 641–656.

[13] M. Zheng, G. Ni, Approximation strategy based on the T-product for third-order quaternion tensors with application to color video compression, Appl. Math. Lett. 140 (2023) 108587.
[14] F.L. Hitchcock, The expression of a tensor or a polyadic as a sum of products, J. Math. Phys. 6 (1–4) (1927) 164–189.
[15] L.R. Tucker, Some mathematical notes on three-mode factor analysis, Psychometrika 31 (3) (1966) 279–311.
[16] D. Goldfarb, Z.T. Qin, Robust low-rank tensor recovery: Models and algorithms, SIAM J. Matrix Anal. Appl. 35 (1) (2014) 225–253.
[17] T.G. Kolda, B.W. Bader, Tensor decompositions and applications, SIAM Rev. 51 (3) (2009) 455–500.
[18] Q. Gu, H. Gui, J. Han, Robust tensor decomposition with gross corruption, in: Proc. NIPS, vol. 27, 2014.
[19] R. Tomioka, T. Suzuki, K. Hayashi, H. Kashima, Statistical performance of convex tensor decomposition, in: Proc. NIPS, vol. 24, 2011.
[20] M. Kilmer, K. Braman, N. Hao, R. Hoover, Third-order tensors as operators on matrices: A theoretical and computational framework with applications in imaging, SIAM J. Matrix Anal. Appl. 34 (1) (2013) 148–172.
[21] Z. Zhang, S. Aeron, Exact tensor completion using t-SVD, IEEE Trans. Signal Process. 65 (6) (2017) 1511–1526.
[22] X. Liu, J. Hou, J. Peng, H. Wang, D. Meng, J. Wang, Tensor compressive sensing fused low-rankness and local-smoothness, in: Proc. AAAI, vol. 37, (no. 7) 2023, pp. 8879–8887.
[23] A. Wang, Z. Jin, G. Tang, Robust tensor decomposition via t-SVD: Near-optimal statistical guarantee and scalable algorithms, Signal Process. 167 (2020) 107319.
[24] M. Kilmer, C. Martin, Factorization strategies for third-order tensors, Linear Algebra Appl. 435 (3) (2011) 641–658.
[25] Z. Lin, M. Chen, Y. Ma, The augmented Lagrange multiplier method for exact recovery of corrupted low-rank matrices, 2013, Arxiv: arXiv:1009.5055v3.
[26] Z. Wang, A.C. Bovik, H.R. Sheikh, E.P. Simoncelli, Image quality assessment: From error visibility to structural similarity, IEEE Trans. Image Process. 13 (4) (2004) 600–612.